China Ocean Engineering, Vol.19, No.4, pp.671 – 680

Experimental Study of Pore Pressure and Deformation of Suction Bucket Foundations Under Horizontal Dynamic Loading

LU Xiao-bing (鲁晓兵)[a], WANG Shu-yun (王淑云)[a], ZHANG Jian-hong (张建红)[b], SUN Guo-liang (孙国亮)[b] and SHI Zhong-min (时忠民)[c]

[a] *Institute of Mechanics, Chinese Academy of Sciences, Beijing 100080, China*

[b] *Hydraulic Department, Tsinghua University, Beijing 100084, China*

[c] *Research Center, Chinese Ocean Oil Co., Beijing 100027, China*

(Received 25 May 2005; accepted 8 October 2005)

ABSTRACT

Centrifuge experiments are carried out to investigate the responses of suction bucket foundations under horizontal dynamic loading. The effects of loading amplitude, the size of the bucket and the structural weight on the dynamic responses are investigated. It is shown that, when the loading amplitude is over a critical value, the sand at the upper part around the bucket softens or even liquefies. The liquefaction index (excess pore pressure divided by initial effective stress. In this paper, the developmental degree of excess pore pressure is described by liquefaction index) decreases from the upper part to the lower part of the sand foundation in the vertical direction and decreases from near to far away from the bucket's side wall in the horizontal direction. Large settlements of the bucket and the sand around the bucket are induced by the horizontal dynamic loading. The dynamic responses of the bucket of a smaller height (when the diameter is the same) are heavier. A cyclic crack some distance near the bucket occurs in the sand.

Key words: *centrifuge experiments*; *suction bucket*; *horizontal dynamic loading*

1. Introduction

In recent years, suction bucket foundations have been applied increasingly often in offshore engineering (Clukey *et al.*, 1995; Allersma *et al.*, 1997, 2000). The first advantage of the suction bucket foundation is the convenient method of installation and repeated use. For example, a suction bucket foundation with a diameter of 9 m and a height of 10 m can be installed in 1 ~ 3 hours, with only a pump. The second advantage is that it may mobilize a significant amount of passive suction during uplift. Despite the fact that some studies have been conducted on the installation and static bearing capacity, the details of the responses of the suction bucket foundation under dynamic loadings have remained unknown (Senpere and Auvergne, 1982; Aas and Andersen, 1992; Dyme and Houlsby, 1998). The dynamic loading condition is significant when suction buckets are used as the foundation of a platform. Wave loading and ice-induced dynamic loading cause the foundation to be subjected to cyclic loadings (Tjelta *et al.*, 1990; Bye *et al.*, 1995). The lack of experience in these loading conditions led to a proposal for a test program intended to gain a deeper understanding. The considerable

* This study program is supported by the fund of the Chinese Ocean Oil Co. and the Chinese Academy of Sciences, KJCX2-SW-L03-01 (40025103) and the National Natural Science Foundation of China (Grant No. 10202024)

1 Corresponding author. E-mail: xblu@imech.ac.cn

cost and time consuming nature of prototype tests mean that the investigation of the bearing capacity of prototype devices under different circumstances is of limited practicality. It is much easier to change parameters in small scale tests. Nevertheless, the problem arises concerning the stress-dependent behavior of soil that the measured loadings are so low that measurements are not sufficiently accurate to visualize differences in design. These restrictions can be overcome if the tests are performed in a geotechnical centrifuge. In a centrifuge the soil stresses over a similar depth are the same as in the prototype situation. For example, at 100 g (100 times the Earth's gravity), a suction bucket foundation of a diameter 9 m and a height of 9 m may be simulated with a foundation of a diameter of 0.09 m and a height of 0.09 m.

The ice-induced horizontal dynamic loading is the governing loading for platform in the Bohai Bay in China, while the wave-induced horizontal dynamic loading is the governing loading for the South China Sea. The horizontal dynamic loading is transmitted to the soils by platform and causes the degradation of strength and modulus of the soils. As a result, the bearing capacity of bucket foundations decreases. Therefore, it is important and necessary to clarify the dynamic behavior of bucket foundations under these types of horizontal loadings so that a practical design method and parameters can be provided (Ding *et al.*, 2003; Lu *et al.*, 2003).

In this paper, attention is concentrated on the horizontal cyclic behavior of suction bucket foundations. The effects of the loading amplitude, the size of the bucket and the structural weight on the soil behavior are mainly investigated.

2. Preparation of the Experiments

The experiments are performed in a 50g-tons centrifuge in Tsinghua University. The maximum of the centrifuge's acceleration is 200g. The payload is 250 kg under 200g.

The inner size of the model tank adopted in the experiments is 600 mm × 350 mm × 350 mm. The experimental material is fine sand with specific gravity 2.69, average grain diameter (D_{50}) 0.14 mm and permeability coefficient 5×10^{-4} cm/s. The layout of the experiments is shown in Fig. 1. Three sizes of steel model buckets are used in the centrifugal tests, i.e. 48, 72 and 90 mm inner height with a 60 mm inner diameter. The thickness of both the wall and the top cap is 2.0 mm. A fine pipe of an 8 mm inner diameter and 10 mm length is welded at the center of the top cap. A sliding groove is connected with the pipe closely, allowing a ball to move up and down to adapt to settlement of the bucket. One end of a steel pole is jointed with a ball, and the other end of the pole is connected with the electromagnetic vibration exciter. Thus the pole cannot be dragged when the bucket settles. Two LVDTs (linear variable differential transformers) are located at the top of the fine pipe to measure the vertical and horizontal displacement respectively (Fig. 1). The other two LVDTs are located on the sand surface to measure the settlements of the sand surface at different positions. Ten PPTs made in Druck Co. (English), are buried in the sand around and in the bucket (Fig. 2). The PPTs are not fixed but suspended in the sand.

For the desired uniform density of the sand in the bucket, the sand specimen is divided into mul-

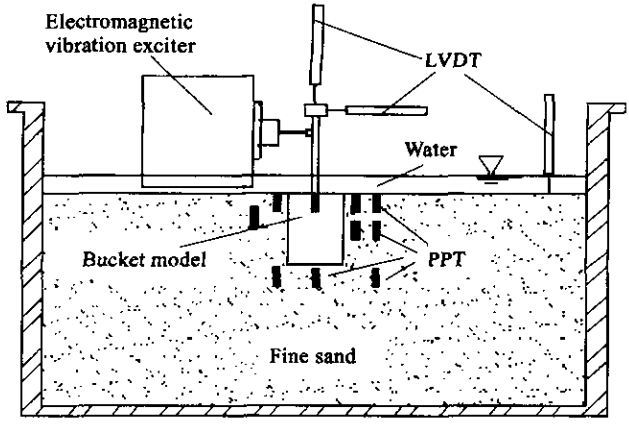

Fig. 1. Layout of the model.

tiple layers according to the layout of PPT, and each layer is compacted gently by hand striking. The water level is 1cm above the sand surface.

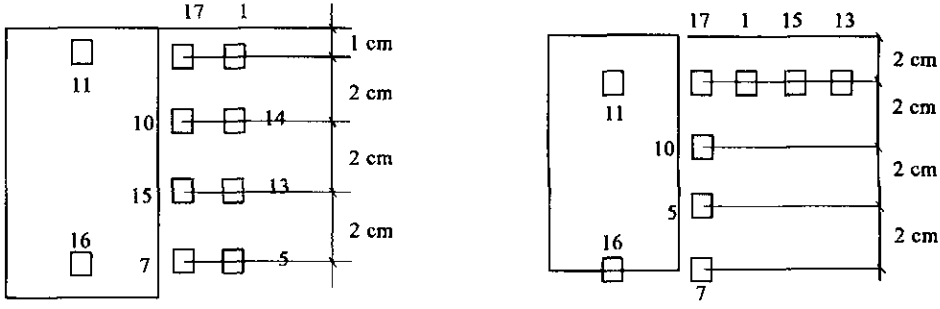

Fig. 2. Layout of the pore water pressure transducers.

After the dry sand sample has been prepared, the sand layer is saturated by filling water from the bottom of the tank through a valve. A 2 cm thick coarse sand layer is laid at the bottom of the tank to allow the water to rise uniformly and prevent piping. When the water level is over the sand surface, vacuum in the sand is applied for 38 hours to increase the saturation degree.

After saturation is completed, consolidation is performed under a consolidation pressure of 80g. The dry densities before and after consolidation are 1.52 g/cm^3 and 1.6 g/cm^3, respectively. The buoyant unit density is $\gamma' = 9.71$ kN/m^3 and the settlement is 0.8 cm after consolidation. The consolidation curves are presented in Fig. 4a.

Ten Pore Pressure Transducers (PPT) are buried in the sand around and inside the bucket. The layout of PPT in the tests are shown in Fig. 2.

A cyclic dynamic loading is adopted in the experiments, for the convenience of investigating the responses of bucket foundations under main frequencies. The loading point is at 8 cm above the top of the bucket at the beginning. But this relative position will change a little with the development of the

settlement. Steel blocks with different weights are located at the top of the fine steel pipe to simulate the effects of the structural weight. A typical loading characteristic is shown in Fig. 3.

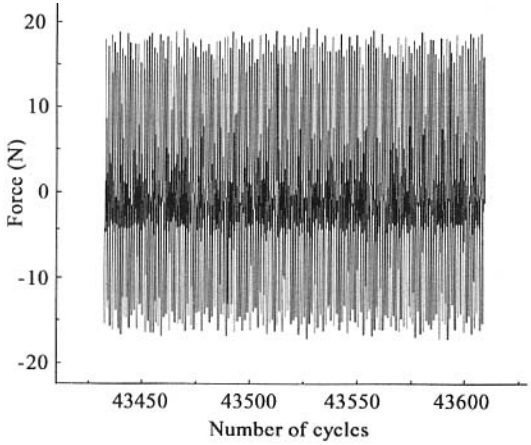

Fig. 3. Loading characteristics.

3. Experimental Results

3.1 Reliability of the Experimental Data

For the reliability of the test data, some tests are repeated three or more times. Fig. 4 shows the reliability of the test results for the 60 mm inner diameter and 72 mm height bucket with the loading amplitude of 60 N and the frequency of 1 Hz. The development of liquefaction index along the depth of the sand foundation is shown in Fig. 4b.

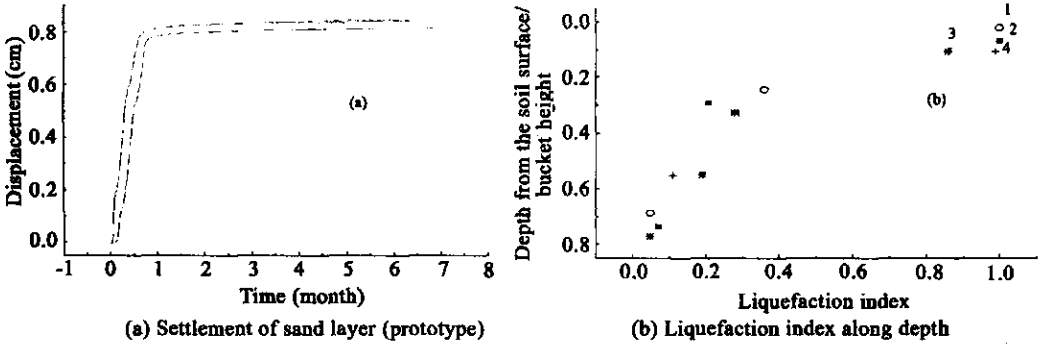

Fig. 4. Reliability of the experimental results.

3.2 Effects of Loading Amplitude

Under the applied dynamic loadings, the liquefaction index increases at the first stage and then decreases. The effects of loading amplitude (e.g. liquefaction index excess pore pressure divided by initial effective stress, settlement) are shown in Figs. 5 ~ 7.

The maximum of the liquefaction index increases with the increase of the loading amplitude (Fig. 5). It is obvious that the disturbance that the sand bears will increase with the increase of the applied

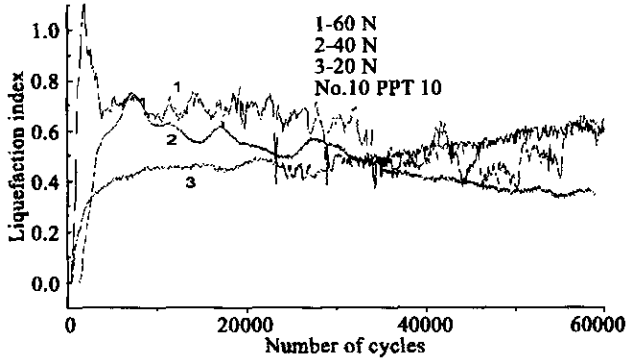

Fig. 5. Liquefaction index vs. time for different loading amplitudes (No. 10).

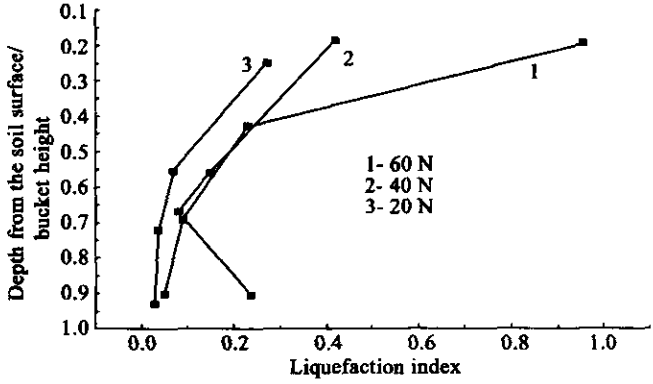

Fig. 6. Liquefaction index vs. loading for different loading amplitudes. (The values of PPTs at the first rank are adopted)

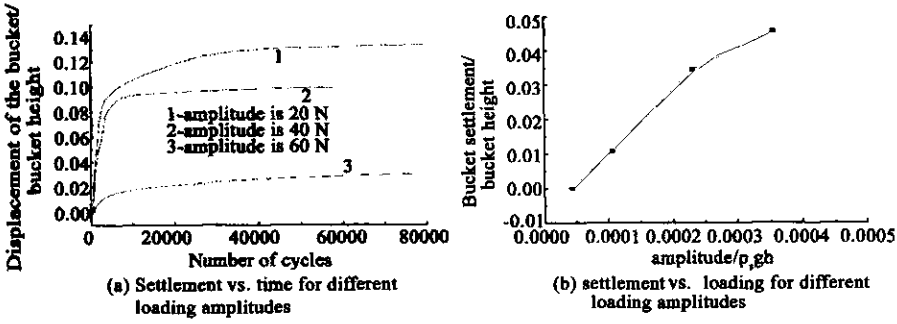

Fig. 7. Settlements of the bucket.

loading, therefore the liquefaction index increases fast and high. With the increase of the loading amplitude, the liquefaction index at each point in the sand increases (Fig. 6).

The development of settlement under different loading amplitudes is shown in Fig. 7. When the

loading amplitude is over a critical value, settlement occurs. Generally, the settlement develops fast at the first stage and gradually arrives at a maximum. The settlement becomes smaller and smaller when the loading amplitude changes from 60 N to 20 N. When the amplitude is 10 N, no settlement occurs.

It is obvious that, at the first stage, the pore water is difficult to drain, so the liquefaction index increases. The strength of the sand decreases with the increasing liquefaction index. Once this condition occurs, the drainage and consolidation becomes fast, that is, the diffusion of excess pore pressure is over the generation. Accordingly, the sand settles and the pore pressure decreases.

3.3 Effects of Loading Frequency

Figs. 8 and 9 show the development of liquefaction index under different loading frequencies. The test results indicate that the liquefaction index increases with the cyclic loading frequency. The excess pore pressure builds up much faster under higher loading frequency (0.8 Hz) than under lower loading frequency (0.4 Hz and 0.2 Hz) shown in Fig. 9. The reason is that the lower the frequency is applied to sand, the better the drainage in the sands.

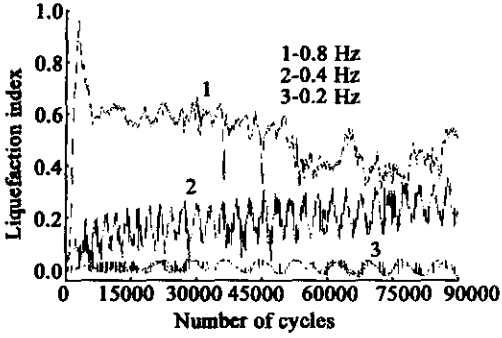

Fig. 8. Effect of loading frequency on liquefaction index.

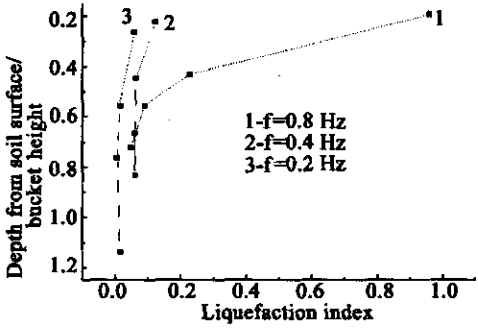

Fig. 9. Effect of loading frequency on liquefaction index.

Fig. 10 shows the effects of loading frequency on the settlement of the bucket. The results indicate that the settlement increases with the cyclic loading frequency. The reason is that the excess pore pressure under higher cyclic loading frequency builds up faster and higher than under lower cyclic loading frequency.

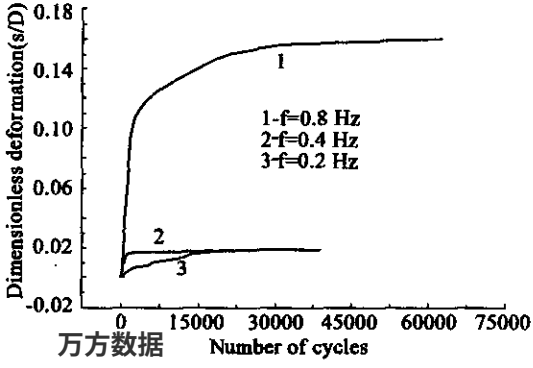

Fig. 10. Effects of loading frequency on settlement of bucket.

3.4 Effects of Bucket Size

The results shown in Figs. 11 and 12 indicate that liquefaction index of sand for a smaller bucket size (6 cm in diameter and 4.8 cm in height) builds up faster and higher than for a larger bucket size (6.0 cm in diameter and 7.2 cm in height). Fig. 13 also shows that the settlement of the smaller size bucket is larger than that of the larger size one under the same loading conditions.

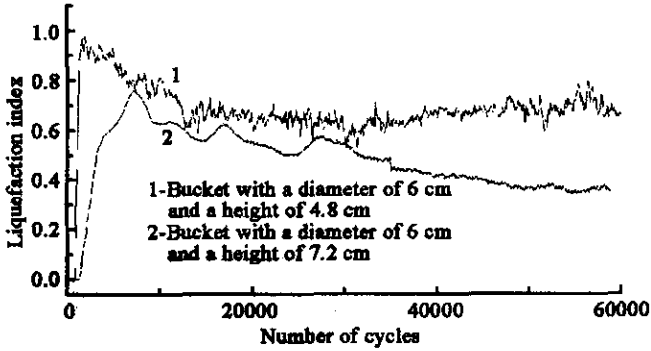

Fig. 11. Liquefaction index vs. number of cycles for different bucket sizes.

Fig. 12. Liquefaction index vs. depth for different bucket sizes.

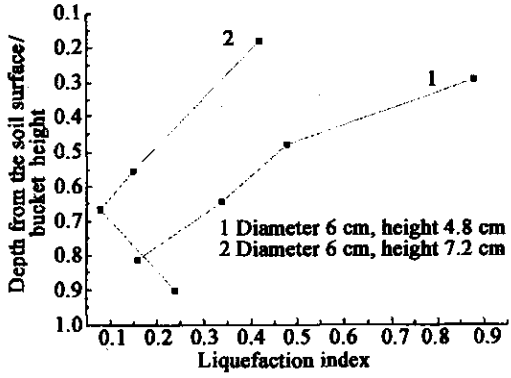

3.5 Results for Different Positions in Sand

The buckets with an inner height of 4.8 and 7.2 cm, and an inner diameter of 6 cm were used for centrifugal tests here. The loading amplitude is 60 N. The results show that the liquefaction index decreases with depth. The sand has been liquefied at a shallow depth. The liquefaction index is only 0.08 at the level of the bottom of the bucket. This may be why the bearing capacity has only reduced a little when the loading lasts for a long time.

In the horizontal direction, the liquefaction index decreases roughly exponentially (Fig. 14). The test shows that the sand has been liquefied under 1200 cycles of 60 N cyclic loading at a depth of 14.4 mm (0.2 bucket height) and 2 mm away from the bucket wall, while the liquefaction index is only 0.4 at 17 mm away from the bucket wall. The settlements of the bucket and the sand 8 cm and 20 cm away from the bucket wall are shown in Fig. 15. It is shown that the settlement decreases radially as a function of the distance from the bucket wall. There is a cyclic crack at some distance near the bucket

(Fig. 16).

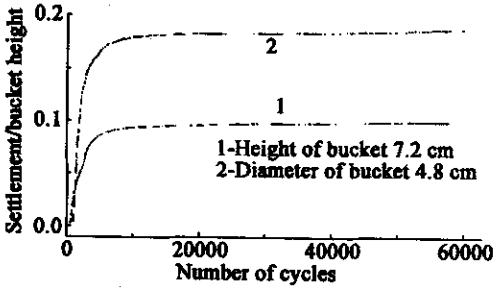

Fig. 13. Settlements vs. number of cycles for the different bucket sizes.

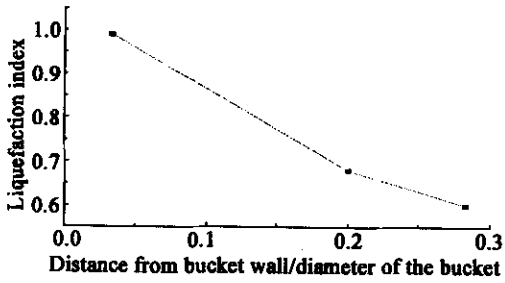

Fig. 14. Largest liquefaction index changes in horizontal direction.

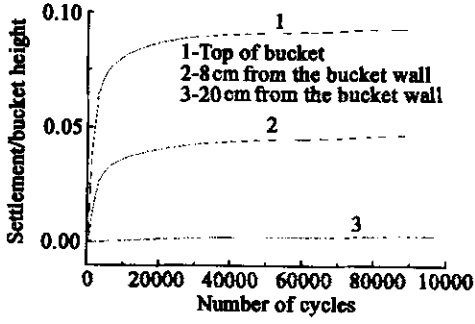

Fig. 15. Comparison of the settlements of the bucket and the sand around.

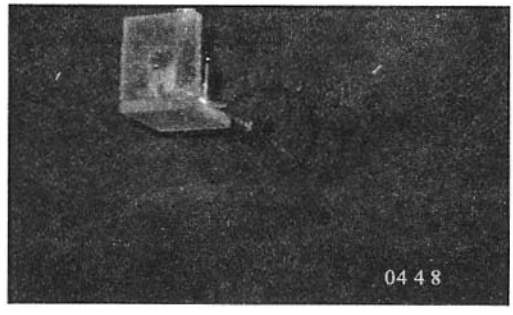

Fig. 16. Cracks after failure of the sand.

3.6 Effects of Structural Weight

The changes of liquefaction index with depth and structural weight are shown in Fig. 17. The results show that the liquefaction index for a bucket with a block is lower than that for a bucket without a block within 28.8 mm from sand surface, but higher below 28.8 mm. The reason is that the increase of the structural weight leads to the increase of the static stress in the sand, and also leads to the increase of the inertial energy of the structure, thus leading to the decrease of the energy transmitted into the sand layer. At the same time, with the changes of the moment of inertial and the center of gravity, the interaction between the bucket and the sand around changes, making the responses become uniform in the vertical direction.

The results of the liquefaction index developing with time at the upper part and at the lower part are shown in Fig. 18. It is shown that at the upper part, the liquefaction index develops faster with a block than without a block. The contrary is the case at the lower part.

The settlement of the bucket with a block is larger than that without a block (Fig. 16). The reason is that the bucket with a block has a larger pressure on the sand, and, when the sand softens under the dynamic loading, larger settlement will occur.

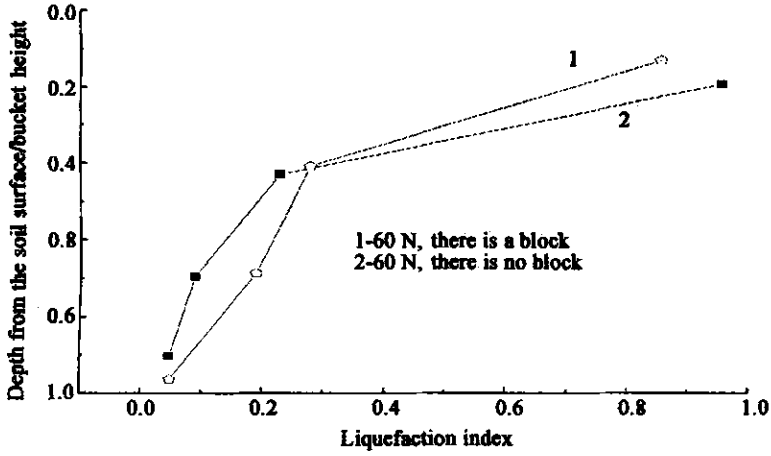

Fig. 17. Liquefaction index vs. depth for different structural weights.

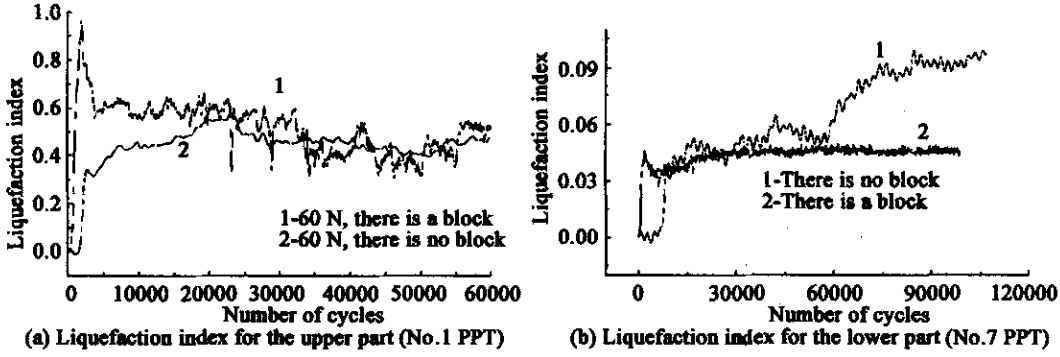

Fig. 18. Liquefaction index vs. time for different structural weights.

Fig. 19. Settlement of bucket for different structural weight.

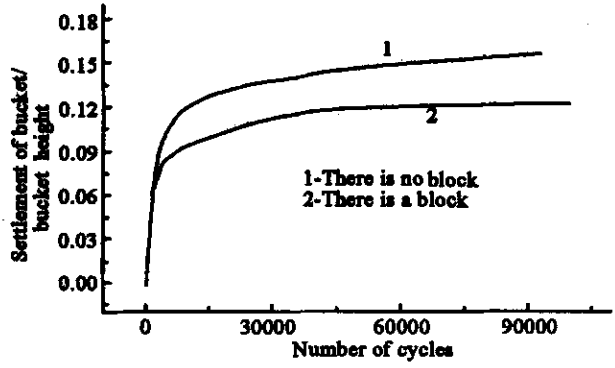

4. Conclusions

Centrifuge experiments are carried out to investigate the responses of bucket foundations under horizontal dynamic loading. It is shown that when the amplitude is over a critical value (in our experi-

ments, the amplitude is about 10% of the static bearing capacity), the sand at the upper part (about 40% of the bucket height) around the bucket softens or even liquefies. Because the sand at the upper part and near the bucket bears more disturbance, the liquefaction index develops faster.

The liquefaction index decreases with depth in the sand foundation and decreases with the distance from the bucket wall in the horizontal direction.

The liquefaction index for a bucket of smaller height (for the same diameter) increases faster than for a bucket of a larger height at every position.

The horizontal dynamic loading induces large settlement of the bucket. The settlement in horizontal direction decreases steadily with the distance from the bucket wall. A cyclic crack near the bucket occurs in the sand.

References

Aas, P. M. and Andersen, K. H., 1992. Skirted foundation for offshore structure, *Proc. of 9th Offshore South East Asia Conf.*, Singapore, 1 ~ 7.

Allersma, H. G. B., Plenevaux, F. J. A. and Wintgens, J. F. P. C. M. E., 1997. Simulation of suction pile installation in sand in a geocentrifuge, *Proc. of 7th Int. Offshore and Polar Engrg. Conf.*, ISOPE97, 1 : 761 ~ 765.

Allersma, H. G. B., Kierstein, A. A. and Maes, D., 2000. Centrifuge modeling on suction piles under cyclic and long term vertical loading, *Proc. Tenth Int. Offshore and Polar Engrg. Conf.*, 2000, Seattle, USA.

Bye, A., Erbrich, C., Earl, K. *et al.*, 1995. Geotechnical design of bucket foundation, *Offshore Technology Conference*, OTC7793, 869 ~ 883.

Clukey, E. C., Morrison, M. J., Garnier, J. *et al.*, 1995. The response of suction caissons in normally consolidated clays to cyclic TLP loading conditions, *Offshore Technology Conference*, OTC 7796, 909 ~ 918.

Ding, H. Y., Qi, L. and Du, X. Z., 2003. Estimating soil liquefaction in ice-induced vibration of bucket foundation, *J. Cold Reg. Eng.*, **17**(2) : 60 ~ 67.

Dyme, W. and Houlsby, G. T., 1998. Drained behavior of suction caisson on very dense sand, *Offshore Technology Conference*, OTC10994, 765 ~ 782.

LU Xiaobing, ZHENG Zhemin and ZHANG Jinlai, 2003. Progress in the study on the bucket foundation of offshore platform, *Advances in Mechanics*, **33**(1) : 27 ~ 40. (in Chinese)

Senpere, D. and Auvergne, G. A., 1982. Suction anchor piles-a proven alternative to driving or drilling, *Offshore Technology Conference*, OTC4206, 483 ~ 493.

Tjelta, T. L., Hermstad, J. and Andenaes, E., 1990. The skirt piled gullfaks c platform installation, *Offshore Technology Conference*, OTC6473, 453 ~ 462.